POLITECNICO DI TORINO
Repository ISTITUZIONALE

Optimization of a Lightweight Gyroid-Based Heat Exchanger for Space Applications

Original
Optimization of a Lightweight Gyroid-Based Heat Exchanger for Space Applications / Diperna, R., Di Benedetto, A., De Palo, S., Giuffrida, F., Lavopa, V., Moretto, M., Puddu, B., Quaranta, A., Savoldi, L.. - ELETTRONICO. - (2025). (6th International Conference on Fluid Flow and Thermal Science (ICFFTS 2025) Barcelona (SPAIN) October 29 - 31, 2025) [10.11159/icffts25.138].

Availability:
This version is available at: 11583/3005491 since: 2025-12-02T09:15:38Z

Publisher:
International ASET Inc.

Published
DOI:10.11159/icffts25.138

Terms of use:

This article is made available under terms and conditions as specified in the corresponding bibliographic description in the repository

Publisher copyright

(Article begins on next page)

17 August 2026

Proceedings of the 6th International Conference on Fluid Flow and Thermal Science (ICFFTS 2025)
Barcelona, Spain - October 29 - 31, 2025
Paper No. 138
DOI: 10.11159/icffts25.138

Optimization of a Lightweight Gyroid-Based Heat Exchanger for Space Applications

Roberto Diperna[1], Andrea Di Benedetto[2], Savino De Palo[2], Federico Giuffrida[3], Vincenzo Lavopa[2], Matteo Moretto[2], Bernardo Puddu[3], Albino Quaranta[2], Laura Savoldi[1]
[1]Dipartimento Energia "Galileo Ferraris", Politecnico di Torino, 10129 Torino, Italy
roberto.diperna@polito.it ; laura.savoldi@polito.it
[2]Thales Alenia Space Italia, 10146, Turin, Italy
savino.depalo@thalesaleniaspace.com ; albino.quaranta@thalesaleniaspace.com;
andrea.dibenedetto@thalesaleniaspace.com ; vincenzo.lavopa@thalesaleniaspace.com;
matteo.moretto@thalesaleniaspace.com ;
[3]CIM4.0 - Competence Center, 10135, Turin, Italy
federico.giuffrida@cim40.com ; bernardo.puddu@cim40.com

Abstract **-** In the framework of human space flights, the active control of temperature inside crewed modules assumes paramount importance in protecting the habitable environment from the harsh thermal conditions of outer space. The need to actively remove the heat from the module is met through suitably sized heat exchangers, as part of the Active Thermal Control Subsystem (ATCS). This requirement must be integrated with the need for lightweight and compact components. A Compact Heat Exchanger (CHX) for space applications, based on Triply Periodic Minimal Structures, namely the gyroid, has been designed and manufactured in metal through additive manufacturing. This paper presents two prototypes of a modular heat exchanger, each composed of nine sequential modules arranged in a counter-flow configuration. The first prototype targets the validation of the modular approach and is manufactured and tested to verify the thermal performance and the heat exchanger conceptual design. The second prototype demonstrates the optimized design and manufacturing of the manifolds and connections among the modules. The thermal performance is assessed experimentally using the efficiency-NTU methodology. Overall, it is demonstrated that the performance of the heat exchanger is consistent with that of an ideal counter-flow one, and that the adopted modular approach allows reaching the expected performance.

Keywords**:** Gyroid; TPMS structures; Heat Exchangers; Additive Manufacturing; Experiment; Space Heating

1. Introduction

In human spaceflight missions, ensuring a stable and safe thermal environment within crewed modules is a critical engineering challenge. The extreme temperature variations in the space environment impose stringent requirements for onboard thermal management systems [1], [2]. Specifically, the Active Thermal Control Subsystem (ATCS) plays an essential role in guaranteeing thermal balance by actively removing excess heat from the habitat and dissipating it into space [3], [4], [5]. The design of ATCS components must therefore meet two requirements often conflicting: achieving high thermal efficiency while maintaining minimal weight and volume, in line with space system constraints [6].

Heat exchangers (HX) are particularly crucial among the ATCS elements, as they directly affect the system ability to effectively transfer and reject heat [7], [8]. Conventional HX designs typically face trade-offs between compactness and thermal performance, limiting their applicability in constrained aerospace environments. In this context, heat exchangers based on Triply Periodic Minimal Surfaces (TPMS), realizable by Additive Manufacturing (AM), represent a promising solution [9], [10]. These structures enable a lighter and more compact architecture while increasing the overall heat exchange surface and therefore providing enhanced performances over a broader temperature range [11], [12], [13]. The gyroid, in particular, is a TPMS structure that lends itself well to metal HX. In its "sheet" form, it splits the volume into two identical fluid channels, enabling high compactness and efficient heat transfer, as demonstrated in multiple recent studies [14], [15]. Lai and Samad (2025) confirmed that gyroid-based HX not only achieve up to 73% improvement in heat transfer rate over conventional plate HXs, but also offer high mechanical strength, low pressure drops, and great adaptability to AM. Notably, their comparative analysis revealed a further performance increase (>6%) when using aluminum over stainless steel, highlighting the potential of integrated material-geometry optimization for aerospace systems [14]. Additional experimental

validation was provided by Kus et al. (2024), who tested a full-scale gyroid HX fabricated via Laser Powder Bed Fusion (LPBF). Their prototype achieved a >10% increase in NTU and 5% improvement in effectiveness compared to a commercial plate HX, despite a 30% reduction in volume. The study further emphasized the structural robustness and reliability of the gyroid lattice under high thermal loads, compact, high-performance thermal systems [15]. Moreover, recent advancements in additive manufacturing technologies have significantly enhanced the feasibility of integrating complex TPMS structures into aerospace-grade components, enabling unprecedented geometrical freedom and high precision [16]. These capabilities facilitate novel HX designs tailored specifically to the rigorous demands of human spaceflight, balancing performance, reliability, and compactness.

Building on these promising findings, the present study introduces a novel modular Compact Heat Exchanger (CHX) concept for space applications, based on gyroid topology and specifically arranged for the AM Laser Powder Bed Fusion (LPBF) technology. The design process for the CHX consists of two phases. Initially, a conceptual design was developed for a modular heat exchanger composed of nine sequential modules arranged in a global counter-flow configuration. A first prototype (D1) is purposely manufactured to validate the modular design concept. Subsequently, a second prototype (D2) is designed and manufactured, again with nine modules, with a specific focus on the manufacturing optimization and engineering of manifold and inter-module connections. Both prototypes have been fabricated by using a common AM aluminum alloy (AlSi10Mg), via metal additive manufacturing (3D printing) and experimentally tested at Thales Alenia Space to evaluate their thermal performance.

2. Geometry

The design of the CHX was driven by both dimensional and performance requirements. Specifically, the overall assembly had to fit within a maximum volume of 750 mm × 250 mm × 250 mm, later reduced to 300 mm × 190 mm × 190 mm, ensuring an efficiency above 90% at a mass flow rate of 0.094 kg/s. The operating conditions involved a cold stream entering at 4 °C and a hot stream at 22 °C. These requirements were defined by considering a fluid belonging to the family of dielectric and low-toxicity, nonflammable HydroFluoroEthers (HFE) fluids. Based on that, a modular design has been developed, where the modules are connected in series, giving globally a counter-flow configuration as shown in Fig. 1

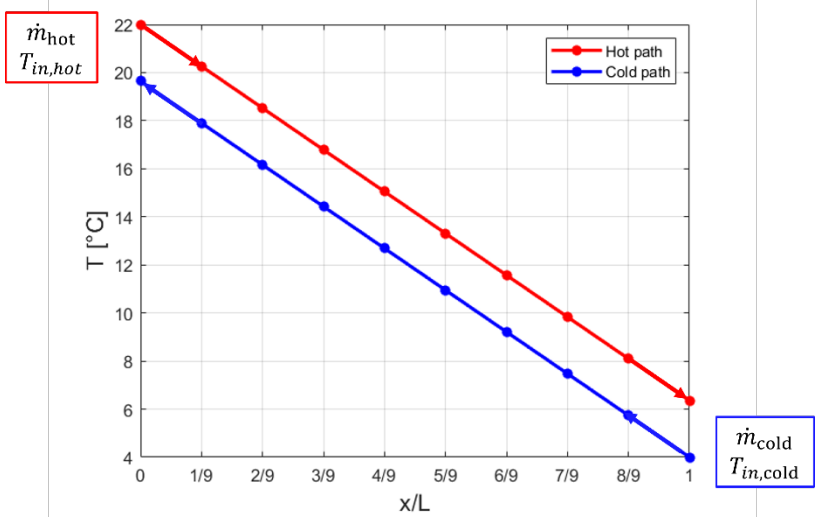

Fig. 1. Temperature profiles along the normalized length of the counterflow HX under design. Identical mass flow rates and fluid properties are assumed for both circuits, resulting in symmetric thermal gradients. The inlet conditions for each stream are indicated at the respective boundaries.

The adoption of a modular design for the heat exchanger (HX) was primarily motivated by performance and manufacturing considerations. From a thermal-fluid dynamic standpoint, a modular layout canes out from an extremization of the baffle

shell-and-tube classical design, restricting the flow area available for the fluids. A series connection of the modules allows achieving higher values of the Reynolds number, which leads to higher heat transfer efficiency.

At the same time, the modular approach offered an effective solution to overcome manufacturing constraints related to the chosen geometry – Triply Periodic Minimal Surfaces (TPMS), specifically gyroids – which can only be produced via additive manufacturing (AM). The limited build volume of available AM systems imposes restrictions on the size of printable components. The post-processing requirements further supported this approach. The internal porosity of TPMS structures poses a significant challenge to de-powdering processes. Additionally, the modular design offers scalability and adaptability for future applications. The trade-off between module size, pressure drop, surface area, and overall efficiency is tightly linked to the minimum gyroid unit cell size that can be reliably printed and de-powdered with current AM technologies. As a beneficial side effect, from a computational perspective, the modular architecture allows for preliminary CFD simulations to be conducted on a single representative module, drastically reducing the computational cost associated with full-system performance evaluations.

A set of parametric simulations was first conducted with the objective of evaluating the relationship between gyroid size and porosity on heat transfer. The configuration that was determined to be optimal was composed of nine modules arranged in a 3 × 3 array, obviously connected in series. Each module was designed to contain a lattice of 10 mm gyroid cells with 1 mm wall thickness (Fig. 2a). The TPMS lattice was generated using the nTop [17] software, while the performance was computed using commercial CFD software [18], [19].

Initially, the entire HX assembly was conceived as a single monolithic block to avoid connections (Fig. 2a, D1). The prototype was fabricated in AlSi10Mg via LPBF. However, due to printing constraints, the wall thickness had to be increased to 2.5 mm, deviating from the optimal value, and the dense 10 mm lattice caused significant issues during de-powdering. These factors ultimately limited the performance of the D1 prototype and revealed the need for a revised strategy. The modular approach was then pushed even more ahead in the design of the second prototype (D2), fabricating the HX in separate modules, enabling then the individual cleaning and de-powdering, which significantly improved the reliability of the process and ensured the proper functionality of the flow paths. The D2 prototype was again manufactured in AlSi10Mg via LPBF (requiring approximately 100 hours of print time for the complete assembly) and consists of nine self-standing modules connected through external piping, sealed with custom “plug & seal” inserts (Fig. 2b).

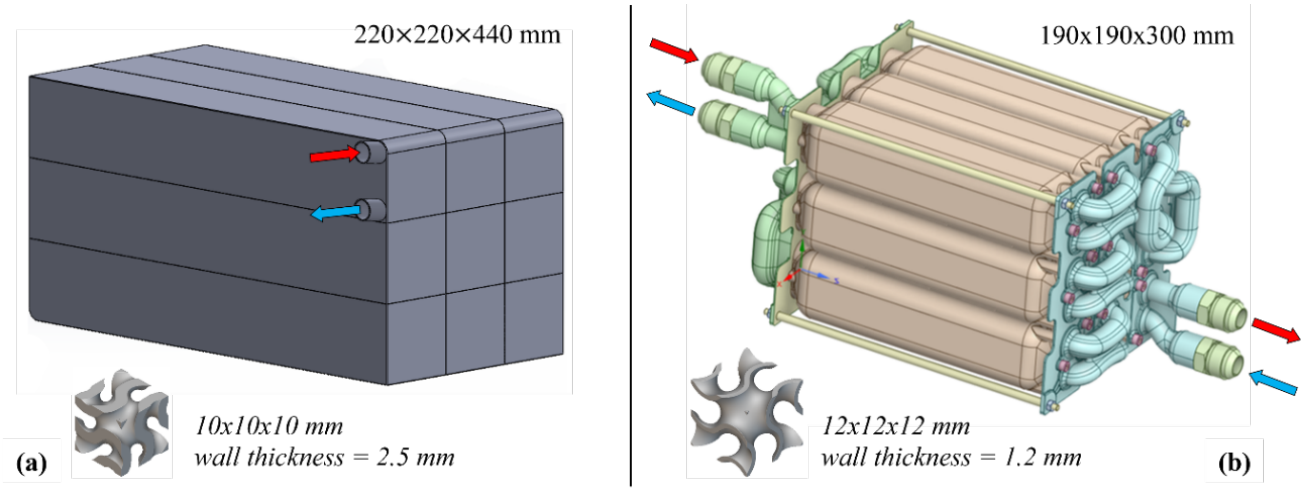

Fig. 2. CHX design: (a) D1 and (b) D2

Surface roughness was improved and de-powdering was facilitated by slightly increasing the gyroid cell size to 12 mm and reducing the wall thickness to 1.2 mm. Additionally, the overall length of the heat exchanger along the flow direction was reduced to approximately two-thirds of that of the D1 prototype, following updates to footprint requirements and to

ensure compliance with the maximum allowable length constraints. In the new D2 design, the TPMS dimensions and wall thickness were designed through mechanical and thermal-fluid dynamic simulations.

3. Experimental campaigns

The entire test campaigns for both CHX prototypes were conducted at the Thales Alenia Space premises in Turin, the first one (D1) in 2024 and the (first module of the) second one (D2) in 2025. Note indeed, while the entire heat exchanger was assessed in the first case, only one module of the D2 was tested due to time constraints. Testing of the complete D2 assembly is currently underway.

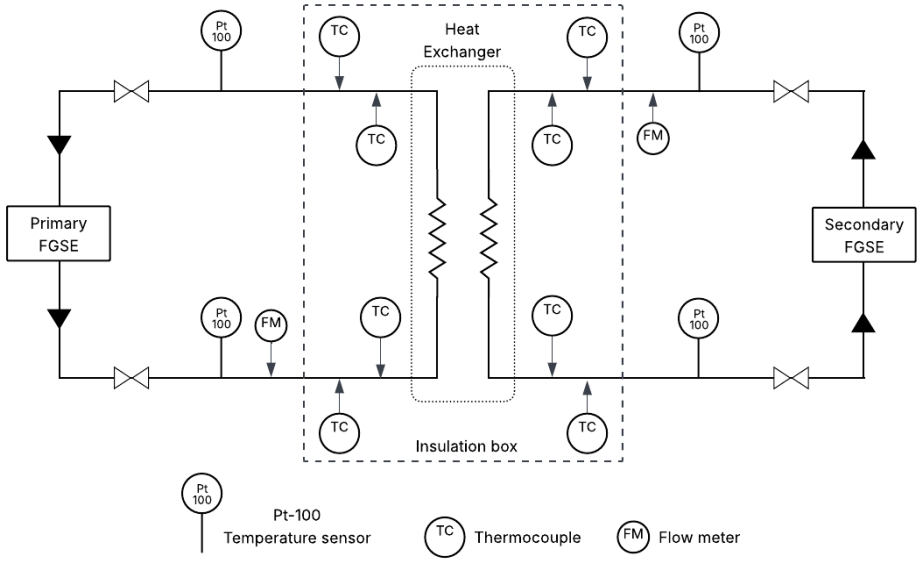

Fig. 3. Sketch of the experimental setup

A sketch of the experimental setup is summarized in Fig. 3, with the following components:

- Two temperature-controlled pumping units (Primary and secondary Fluidic Ground Support Equipment - FGSE): Primary unit is featured by numerous valves, junctions, and an additional heat exchanger to stabilize the fluid temperature at its outlet. This unit is directly connected to a Lauda 4600 chiller, a thermostat that has an adjustable heating and cooling capacity and small, active internal volume that enables fast temperature changes. The internal bath of the chiller has a heating power of approximately 4600 W, supporting a temperature range from -30°C up to 120°C. The opposite side is regulated by a secondary FGSE. These units utilize a solution composed of water and glycol (ethylene glycol for tests conducted on D1 and propylene glycol for those conducted on D2).
- Two digital Flow Meters: the FTB-800 turbine flow meter by Omega transmits an electrical signal to the Data Acquisition System (DAQ), which converts the signal using a linear relationship. Its measurement accuracy is within ±2% for flow rates ranging from 228 l/h to 2274 l/h.
- Four Pt 100 (Class 1/9) Temperature Sensors: these are highly precise wet sensors that should be positioned near the specific region where temperature measurement is needed. During testing, the Pt-100 sensors were located as close as possible to the inlet and outlet sections to accurately evaluate the performance of the heat exchanger (CHX). The measurement accuracy within the specified temperature range is ±0.05°C.
- Eight T-type thermocouples: these sensors were employed solely for redundancy purposes. As dry sensors, they were directly installed at the inlet and outlet sections of the CHX.

Since the experimental results are intended to be as independent as possible of the surrounding conditions, efforts were focused on insulating the heat exchanger before proceeding with the test activities. At first, the heat exchanger was enclosed

in a box made of insulating material. To further enhance insulation from the environment, the empty spaces within the box were filled with small polystyrene spheres, markedly decreasing the air volume inside. Fig. 4 shows the insulation box, where the CHX is contained. The same procedure was carried out for the test on D2 (Fig. 5).

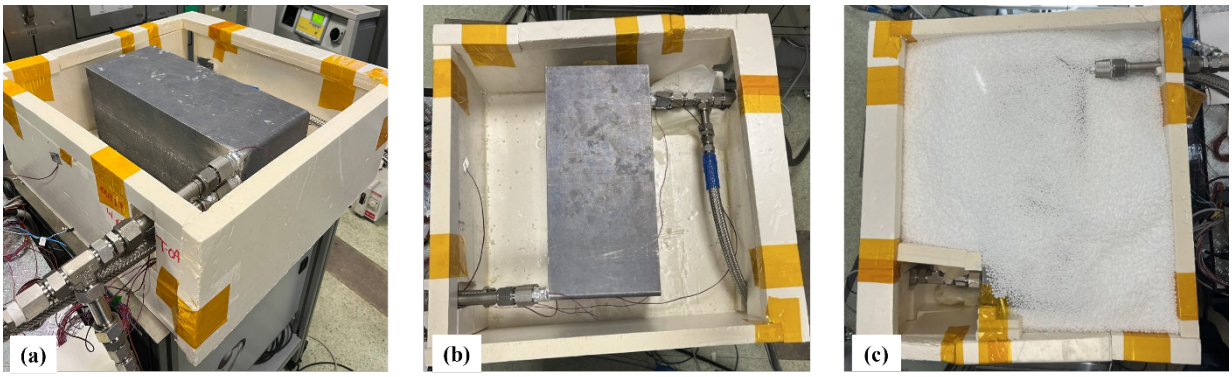

Fig. 4. CHX insulation box for D1: (a) Isometric view (b) Top view, (c) Filled box with polystyrene.

After verifying that the heat exchanger had been insulated properly, it was connected to the control units together with its piping system. Temperature readings, obtained using wet sensors (Pt-100), were recorded at the inlet and outlet sections of the heat exchanger to assess its actual performance. The Data Acquisition System (DAS) was configured to record data at a minimum rate of 1 Hz. Data were appropriately averaged over a minimum of 2 minutes following the signal stabilization.

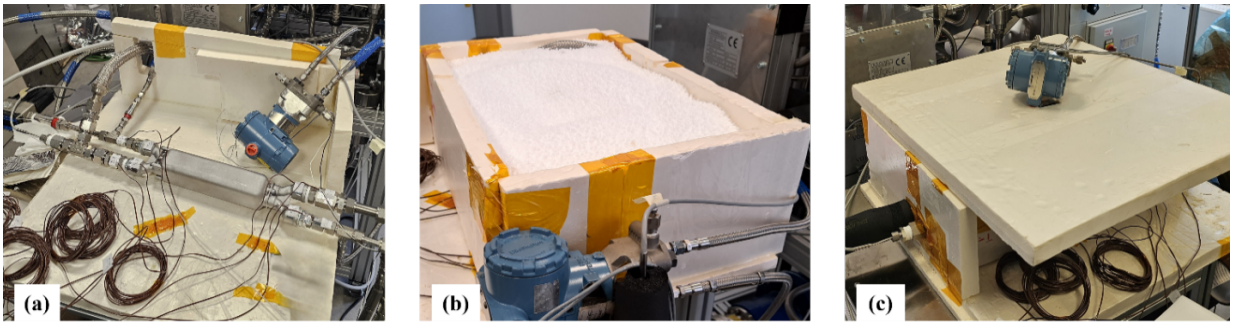

Fig. 5. CHX insulation box for D2: (a) Top view, (b) Filled box with polystyrene, (c) Closed box

3. Results and discussion

Regarding thermal performance, the computed and measured data are analyzed in terms of the efficiency ε (Eq. 1) as a function of the Number of Thermal Units (*NTU*) in Eq.2 [20].

$$\varepsilon = \frac{0.5 * (\Phi_1 + \Phi_2)}{\min\left(\dot{m}_{hot} * c_{p,hot}, \dot{m}_{cold} * c_{p,cold}\right) | T_{in,hot} - T_{in,cold}|} \quad (1)$$

$$NTU = \frac{HA^*}{\min(\dot{m}_{hot} \cdot c_{p,hot}, \dot{m}_{cold} \cdot c_{p,cold})} \quad (2)$$

In Eq. (1), $\dot{m}_{hot}$ and $\dot{m}_{cold}$ are the mass flow rates of the hot and cold fluid, respectively, having each its specific heat $c_{p,hot}$ and $c_{p,cold}$. The variables $T_{in,hot}$ and $T_{in,cold}$ are the hot and cold fluid inlet temperatures, respectively, whereas Φ_1 and Φ_2

are the thermal power released by the hot fluid and received by the cold fluid, respectively, computed accordingly to Eqs. 3 and 4:

$$\Phi_1 = \dot{m}_{hot} \cdot c_{p,hot} \cdot \left| T_{out,hot} - T_{in,hot} \right| \tag{3}$$

$$\Phi_2 = \dot{m}_{cold} \cdot c_{p,cold} \cdot \left| T_{out,cold} - T_{in,cold} \right| \tag{4}$$

The global heat transfer coefficient (HA^*) in Eq. 5 must be calculated based on the heat flux and the mean logarithmic temperature difference ΔT_{LM}, computed as in Eq. 6 for counterflow HX, according to the value of the heat capacity ratio C_r, defined in Eq. 8. The hot and cold fluid outlet temperatures are $T_{out,hot}$ and $T_{out,cold}$, respectively.

$$HA^* = \frac{0.5 \cdot (\Phi_1 + \Phi_2)}{\Delta T_{LM}} \tag{5}$$

$$\begin{cases} \Delta T_{LM} = \dfrac{(T_{in,hot} - T_{out,cold}) - (T_{out,hot} - T_{in,cold})}{\ln\left(\dfrac{T_{in,hot} - T_{out,cold}}{T_{out,hot} - T_{in,cold}}\right)} & when\ C_r < 1 \\ \Delta T_{LM} = (T_{in,hot} - T_{out,cold}) = (T_{out,hot} - T_{in,cold}) & when\ C_r = 1 \end{cases} \tag{6}$$

For a perfectly counterflow heat exchanger, the ideal behavior is described by Eq. 7 (where C_r represents the heat capacity ratio defined in Eq. 8).

$$\begin{cases} \varepsilon = \dfrac{1 - \exp[-NTU(1 - C_r)]}{1 - C_r \exp[-NTU(1 - C_r)]} & (C_r < 1) \\ \varepsilon = \dfrac{NTU}{1 + NTU} & (C_r = 1) \end{cases} \tag{7}$$

$$C_r = \frac{C_{min}}{C_{max}} = \frac{\min(\dot{m}_{hot} c_{p,hot}, \dot{m}_{cold} c_{p,cold})}{\max(\dot{m}_{hot} c_{p,hot}, \dot{m}_{cold} c_{p,cold})} \tag{8}$$

As previously noted, only one module of the D2 exchanger was evaluated. An estimate of the heat exchanger's overall performance was obtained by extrapolating the results, specifically by multiplying the heat transfer area, from Eq. 2, by the number of modules, under the assumption that the modules are identical. Using Equation 2, the total *NTU* was calculated, and subsequently, Equation 7 was employed to determine the extrapolated overall efficiency of the complete heat exchanger.

The test campaign results are illustrated in Fig. 6 for both prototypes, with also the expected performance based on the ideal behavior of Eq. 7. For the D1, the experimental evidence proves that for any tested values of C_r, the behavior of the HX is perfectly reproduced by the ideal curve of Eq. 7, even if it must be recognized that the uncertainty bars are pretty large. Also, the test of the single module of D2 behaves as expected, and the modular CHX should achieve global efficiency >80%. If a target efficiency >90% is to be reached, it is straightforward to move in perspective in the direction of further increasing the heat transfer surface (with longer modules, for instance), that allow moving on the ideal curve in Fig. 6b in the direction of increased NTU values. Furthermore, the heat transfer coefficient could also be increased by reducing the original lattice cell size towards the 10 mm value of D1, leading to a further increase of the NTU value. Anyway, the D2 lattice cell size should be kept, to avoid problems during the de-powdering step, with the currently adopted de-powdering procedure.

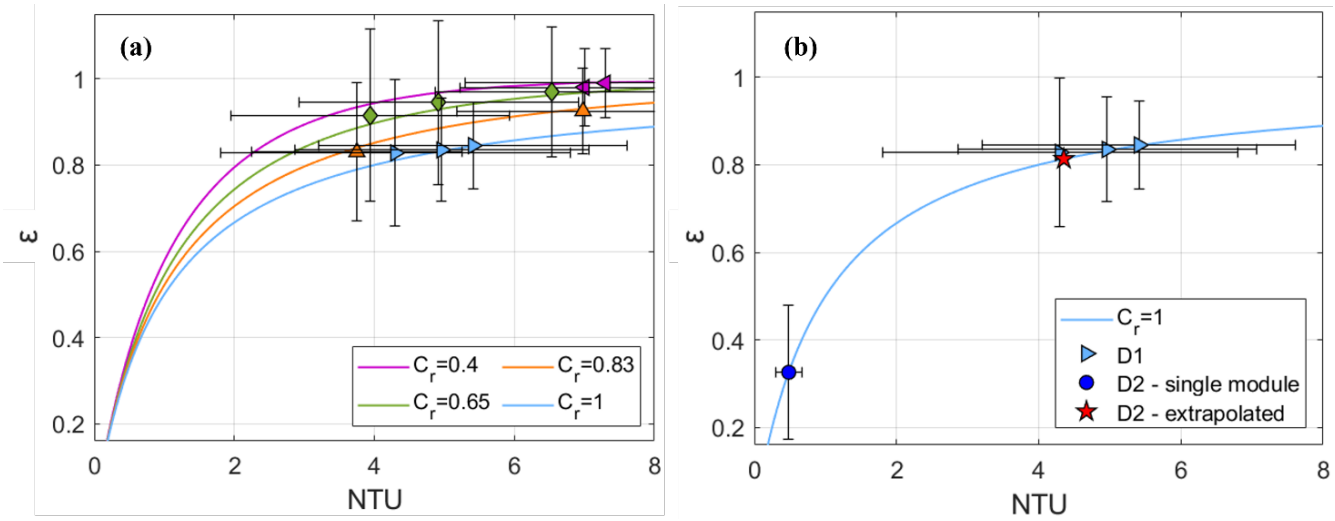

Fig. 6. Measured performance (solid symbols) for the CHXs, compared to the expected values for an ideal counterflow heat exchanger (colored lines). (a) Performance of the first prototype (D1) at various C_r. (b) Comparison of experimental results at C_r=1, between D1 and D2.

5. Conclusion and perspective

The work presented in this paper demonstrates the viability and maturity of the design and manufacturing of a modular Compact Heat Exchanger (CHX) based on Triply Periodic Minimal Surfaces (TPMS), specifically the gyroid topology, for space applications. The experimental results obtained with the first prototype (Design D1), manufactured with a unit cell of 10 mm and wall thickness of 2.5 mm ensuring robustness, confirm the effectiveness of the modular approach, validating both the thermal performance and the underlying heat exchanger concept. The second prototype (Design D2), solving some issues linked to de-powdering, further proves that the engineering of the manifolds and inter-module connections is sufficiently mature to support the development of a fully functional TPMS-based heat exchanger. For both prototypes, the overall measured thermal behavior is consistent with that of an ideal counter-flow heat exchanger, confirming that the TPMS-based design can meet the target performance requirements. These results collectively indicate that the proposed solution is technically sound and sufficiently mature for further integration into space-grade thermal management systems.

References

[1] S. Tachikawa, H. Nagano, A. Ohnishi, e Y. Nagasaka, «Advanced Passive Thermal Control Materials and Devices for Spacecraft: A Review», *Int. J. Thermophys.*, vol. 43, fasc. 6, p. 91, apr. 2022, doi: 10.1007/s10765-022-03010-3.

[2] David G Gilmore e The Aerospace Corporation D Gilmore, *Spacecraft Thermal Control Handbook, Volume I: Fundamental Technologies*, 2nd ed. AIAA (American Institute of Aeronautics & Astronautics), 2002. Consultato: 21 giugno 2025. [Online]. Disponibile su: https://arc.aiaa.org/doi/book/10.2514/4.989117

[3] G. C. Birur, G. Siebes, T. D. Swanson, e E. I. Powers, «Spacecraft Thermal Control», 5 gennaio 2001. Consultato: 21 giugno 2025. [Online]. Disponibile su: https://ntrs.nasa.gov/citations/20010091676

[4] P. Bellmore, «Integrated Active Thermal Control System Analysis of Space Station Freedom Operational Scenarios», *SAE Trans.*, vol. 102, pp. 1247–1254, 1993.

[5] M. Rui, L. Shibin, W. Zhongwei, e W. Lin, «Study on Heat Transfer Mechanism of Active and Passive Thermal Control Structure in Aerospace Vehicle», in *2024 IEEE 22nd International Conference on Industrial Informatics (INDIN)*, ago. 2024, pp. 1–6. doi: 10.1109/INDIN58382.2024.10774299.

[6] R. C. Consolo e S. K. S. Boetcher, «Chapter One - Advances in spacecraft thermal control», in *Advances in Heat Transfer*, vol. 56, J. P. Abraham, J. M. Gorman, e W. J. Minkowycz, A c. di, Elsevier, 2023, pp. 1–50. doi: 10.1016/bs.aiht.2023.04.001.
[7] M. M. Hasan, L. Khan, V. Nayagam, e R. Balasubramaniam, «Conceptual Design of a Condensing Heat Exchanger for Space Systems using Porous Media», presentato al International Conference On Environmental Systems, lug. 2005, pp. 2005-01–2812. doi: 10.4271/2005-01-2812.
[8] K.-L. Lee, C. Tarau, e N. V. Velson, «Development of a Heat Exchanger with Integrated Thermal Storage for Spacecraft Thermal Management Applications».
[9] C. Pérez e A. Revuelta, *Modelling of a Compact Heat Exchanger With TPMS Geometry*. 2025.
[10] K. Dutkowski, M. Kruzel, e K. Rokosz, «Review of the State-of-the-Art Uses of Minimal Surfaces in Heat Transfer», *Energies*, vol. 15, fasc. 21, Art. fasc. 21, gen. 2022, doi: 10.3390/en15217994.
[11] F. L. Rashid, Najah M.L. Al Maimuri, Mudhar A. Al-Obaidi, Muhammad Asmail Eleiwi, Arman Ameen, Shabbir Ahmad, Atef Chibani, Mohamed Kezzar, Ephraim Bonah Agyekum, «Enhancing heat transfer across applications with triply periodic minimal surface (TPMS) structures: A comprehensive review», *Chem. Eng. Process. - Process Intensif.*, vol. 216, p. 110460, ott. 2025, doi: 10.1016/j.cep.2025.110460.
[12] R. Min, Z. Wang, H. Yang, R. Bao, e N. Zhang, «Heat transfer characterization of waste heat recovery heat exchanger based on flexible hybrid triply periodic minimal surfaces (TPMS)», *Int. Commun. Heat Mass Transf.*, vol. 157, p. 107760, set. 2024, doi: 10.1016/j.icheatmasstransfer.2024.107760.
[13] L. K. Dharmalingam, V. Aute, e J. Ling, «Review of Triply Periodic Minimal Surface (TPMS) based Heat Exchanger Designs», 2022.
[14] W.-H. Lai e A. Samad, «Development and flow optimization of "Gyroid" based additive manufacturing heat exchanger: Both computational and experimental analyses», *Int. J. Therm. Sci.*, vol. 213, p. 109835, lug. 2025, doi: 10.1016/j.ijthermalsci.2025.109835.
[15] K. Kus, M. Wójcik, Z. Malecha, e Z. Rogala, «Numerical and experimental investigation of the gyroid heat exchanger», *Int. J. Heat Mass Transf.*, vol. 231, p. 125882, ott. 2024, doi: 10.1016/j.ijheatmasstransfer.2024.125882.
[16] I. Gibson, D. Rosen, B. Stucker, e M. Khorasani, *Additive Manufacturing Technologies*. Cham: Springer International Publishing, 2021. doi: 10.1007/978-3-030-56127-7.
[17] nTopology Inc. 2025, «nTop». [Online]. Disponibile su: https://www.ntop.com/
[18] Siemens Digital Industries Software, «StarCCM +», © Siemens 2025. [Online]. Disponibile su: https://plm.sw.siemens.com/en-US/simcenter/fluids-thermal-simulation/star-ccm/
[19] Ansys, «Ansys Fluent», @2025 Copyright ANSYS, Inc. [Online]. Disponibile su: https://www.ansys.com/products/fluids/ansys-fluent
[20] F. P. Incropera, D. P. DeWitt, T. L. Bergman, e A. S. Lavine, A c. di, *Introduction to heat transfer*, 6. ed. Wiley, 2013.